Version 0.2

Ezio.Todesco@cern.ch

Chapter 4

How to design dipole and quadrupole magnets with current lines

Plan of the chapter

A few coil lay-outs provide a perfect dipolar field; in the first section we describe these configurations, computing the field as a function of the geometrical parameters, and discussing the possible use for magnet design. However, a more powerful model can be used: the approximation based on sector coils. We describe this configuration in Section 4.2, giving the main dependence of the field on the coil width, and in Section 4.3 we discuss how to optimize field quality with few wedges at the level required for accelerator magnets. A system of equations can be derived to solve the field quality optimization, and this allows having an understanding of the reasons for the layout of several dipole cross-sections. In Section 4.4 we show how the sector coil can be used to benchmark the efficiency of any coil layout, making comparisons to the ideal layouts based on intersecting ellipses; moreover we introduce the most optimized layout found with numerical methods. The efficiency of block and double helix layouts are discussed in section 4.6.. In Section 4.7 we consider the field quality optimization for a quadrupole, showing that the equations and the solutions can be derived by a simple rescaling of the dipole case. We conclude this chapter with some comments on how to carry out field quality optimization.

4.1 Lay-outs generating perfect dipole fields

In an infinte solenoid of width w and overall current density j (see Fig. 4.1), the magnetic field is given by

$$B = \mu_0 j w \,. \tag{4.1}$$

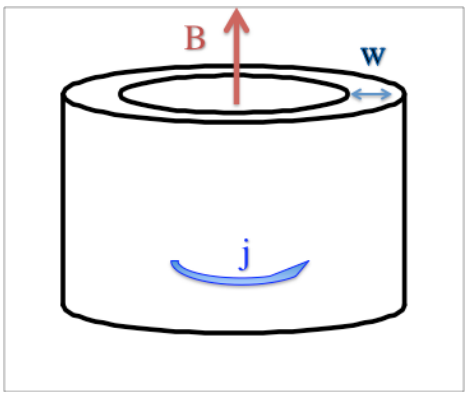

Fig. 4.1: Solenoid configuration, winding width, and field direction.

Note that by overall current density we denote the current density in the insulated coil. Using the practical units of mm for the solenoid width and A/mm^2 for the current density, one has

$$B\left[\mathrm{T}\right] = 4\pi 10^{-4}\, j\left[\mathrm{A/mm^2}\right] w\left[\mathrm{mm}\right] \approx 0.00126\, j\left[\mathrm{A/mm^2}\right] w\left[\mathrm{mm}\right]. \qquad (4.2)$$

This implies that each 10 mm of coil width with 400 A/mm^2 overall current density gives ~5 T.

Accelerator dipoles have to provide a field that is not parallel to the beam direction, but perpendicular to it. We will show that this implies a reduction of a factor two of the field given by the same winding width and current density. Let us start with the configuration of two walls of current, of width w and distance $2r$ (see Fig. 4.2). Integrating the contribution of the current lines, one finds

$$B = 2\frac{\mu_0}{2\pi}\int_r^{r+w}\int_{-\infty}^{\infty}\frac{jx}{x^2+y^2}\,dy\,dx = \frac{\mu_0 j}{\pi}\int_r^{r+w} x\int_{-\infty}^{\infty}\frac{dy}{x^2+y^2}\,dx = \frac{\mu_0 j}{\pi}\int_r^{r+w}\int_{-\infty}^{\infty}\frac{dz}{1+z^2}\,dx = \mu_0 jw\,, \qquad (4.3)$$

and the proportionality constant between the field and the width times the current density is as in the solenoid, (see Eq. 4.1). One can prove that the field inside the walls is uniform, and outside is zero. This is the first ideal configuration providing a perfect dipolar field; it is of little interest since the layout has infinite size.

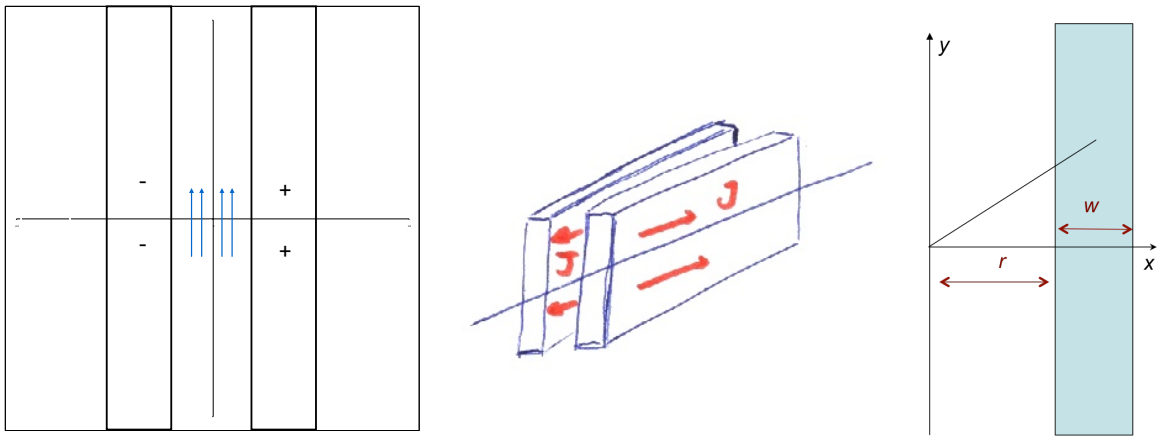

Fig. 4.2: Artist view of the wall dipole (center), cross-section (left), and coordinate system to compute the field (right).

The second case we consider is given by intersecting ellipses (see Fig. 4.3, left). This is a better solution, since the layout is finite, even though the aperture is not round. In this case one can prove (see for instance [1], pg 31) that inside the aperture there is a uniform field, given by

$$B = \mu_0 jw\frac{a_V}{a_H + a_V} \qquad (4.4)$$

where w is the width of the coil in the midplane, a_H is the horizontal semiaxis of the ellipse, and a_V is the vertical semiaxis. In the case of an ellipse with zero eccentricity, i.e. intersecting circles, a_H=a_V and one finds the same expression as in Eq. (4.2).

$$B = \frac{\mu_0 jw}{2} \qquad B\left[T\right] = 0.000628\, j\left[\mathrm{A/mm^2}\right] w\left[\mathrm{mm}\right] \qquad (4.5)$$

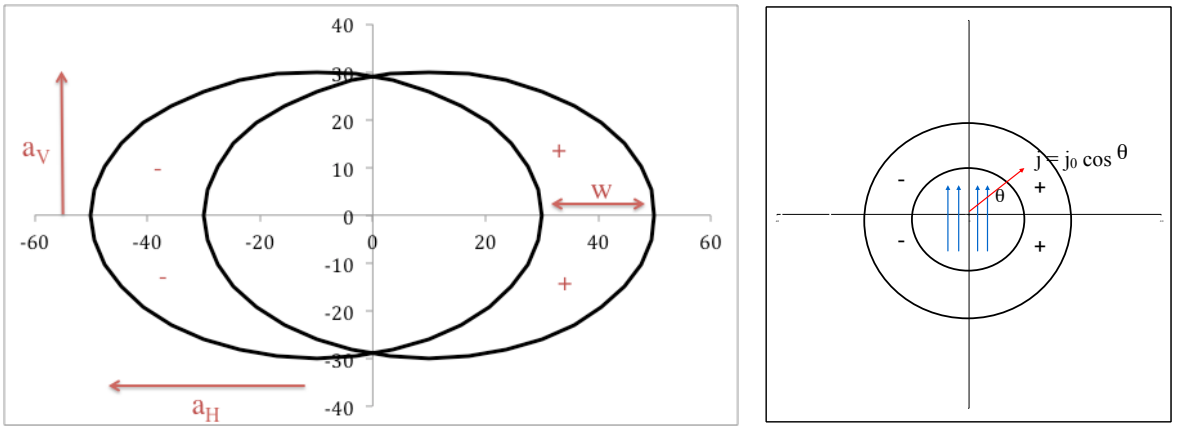

Fig. 4.3: Coil cross-section based on intersecting ellipses (left) and on cos theta current density (right).

The third layout is a ring where the current density depends on the cosine of the angle to the midplane (see Fig. 4.3, right). Here we gain a round aperture, but we lose the uniform current density. Also in this case one has

$$B = 4\frac{\mu_0 j}{2\pi}\int_0^{\pi/2}\int_r^{r+w}\cos^2\theta\, d\theta = 4\frac{\mu_0 j}{2\pi}\frac{\pi}{4}w = \frac{\mu_0 j w}{2} \tag{4.6}$$

where w is the thickness of the ring and j the maximum current density, occurring in the midplane. The cos theta layout has been widely used in the literature to provide analytical estimates of magnet design (see for instance [1,2]). However, a better analytical model can be derived, closer to what is finally achieved during winding: the sector coil [3,4]. This is what we will discuss it in the next section.

We conclude this section by presenting a fourth ideal layout, derived from our starting point (the solenoid): the double helix [5], also know in the literature as tilted solenoid or canted cos theta (CCT). Here the conductor is wound along a solenoid, tilted with an angle α with respect to the beam axis, in two successive layers, with opposite orientation of the angle with respect to the beam direction (see Fig. 4.4). The resulting field inside the aperture is a pure dipole, the aperture is round, and the current density is constant.

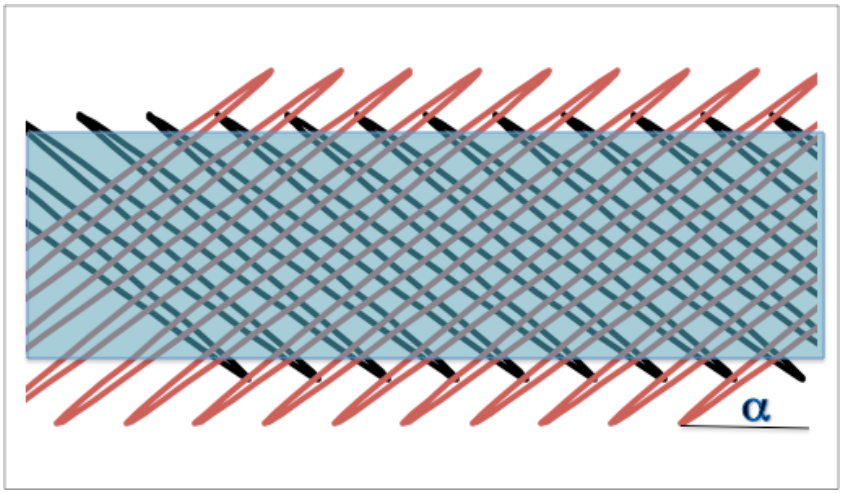

Fig. 4.4: Tilted solenoid configuration, side view with inner winding in black, outer winding in red, and bore tube in blue.

The conductor path is given by the equations parametrized by t

$$\begin{aligned} x(t) &= r\cos t \\ y(t) &= r\sin t \\ z(t) &= pt + r\tan\alpha\sin t \end{aligned} \tag{4.7}$$

where p is the advancement of the spiral along z in each turn. The outer titled solenoid is wound on the outer radius (r+a), with opposite angle α:

$$\begin{aligned} x(t) &= \left(r+a\right)\cos t \\ y(t) &= \left(r+a\right)\sin t \\ z(t) &= pt - \left(r+a\right)\tan\alpha\sin t \end{aligned} \tag{4.8}$$

The rather peculiar shape of the winding can be kept by machining grooves in a supporting structure. The disdvantage of this layout is a lower efficiency, reduced by at least a factor cosα: a fraction of conductor is used to create a solenoidal field that is canceled by the other winding. Typical angles range between 15 and 30 degrees. We give a case study to compute the efficiency of this layout in section 4.4.

4.2 Field in a dipole magnets based on sector coils

We will now analyze a sector coil with windings having a constant current density. Contrary to the wall dipole, the intersepting ellispses and the cos theta, this lay-out is the only one that can be manufactured based on a rectangular cable with a slight keystone to follow the sector shape; the only approximation is that for small apertures (order of 50 mm diameter) as used in arc magnets of very high energy accelerators, the required keystone angle becomes too large and therefore wedges have to be used to arrange the cable stacks perpendicular to the magnet aperture. However, we will show in the next section that a few wedges are anyway needed to get an adequate field quality.

Let us start estimating the main dipolar field given by a sector coil and its efficiency with respect to the solenoid, and to the dipole lay-outs shown in the previous section. The contribution to the magnetic field in the centre (0,0) of the reference system of a line of current I placed in (x_0,y_0) is given by (see Chapter 3)

$$B = -\frac{\mu_0 I}{2\pi}\mathrm{Re}\left(\frac{1}{z_0}\right) = -\frac{\mu_0 I}{2\pi}\frac{\cos\theta}{|z_0|} \qquad z_0 = x_0 + iy_0. \tag{4.9}$$

Replacing the current with current density

$$I \to j\rho d\rho d\theta \tag{4.10}$$

and performing the integration over a sector coil of aperture radius r, coil width w and angular aperture α (see Fig. 4.5) we obtain

$$B = -2\frac{\mu_0 j}{2\pi}\int_{-\alpha}^{\alpha}\int_{r}^{r+w}\frac{\cos\theta}{\rho}\rho d\rho d\theta = -\frac{2\mu_0 j}{\pi}w\sin\alpha\,. \tag{4.11}$$

For a 60° degrees sector coil, one finds the simple expression

$$B = -\frac{\sqrt{3}}{\pi}\mu_0 jw \tag{4.12}$$

and making use of the practical units, one obtains

$$B = -\frac{\sqrt{3}}{\pi}4\pi\times10^{-7}\times10^{6}\, j\left[\mathrm{A/mm^2}\right]10^{-3}\, w\left[\mathrm{mm}\right] \approx 6.9\times10^{-4}\, j\left[\mathrm{A/mm^2}\right] w\left[\mathrm{mm}\right]. \tag{4.13}$$

This gives ~10% higher field with respect to the previous dipole layouts, see Eq. (4.5). If we consider an overall current density j of 400 A/mm^2, each 10 mm of coil width gives 2.8 T of dipolar field. Using this rough estimate for the LHC dipoles, having 30 mm coil width, one finds 8.1 T, close to the actual value of 8.3 T.

Summarizing, one finds that

- The dipolar field is proportional to the current density;
- The dipolar field is independent of the aperture radius r;
- The dipolar field is proportional to the coil width w;
- The 60° degrees sector coil has a 10% larger constant with respect to the ideal cases of a wall dipole, intersecting ellipses or cos theta distribution, where the proportionality constant between field and current density times coil width is μ/2.

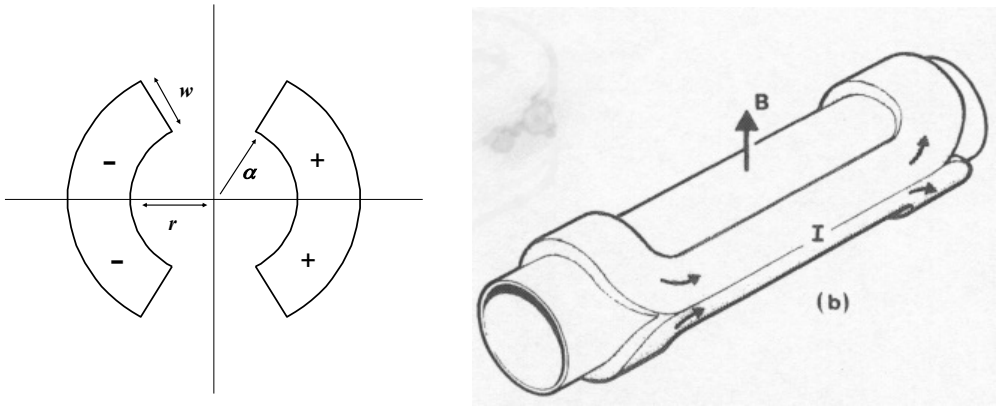

Fig. 4.5: Cross-section of a dipole based on a sector coil (left) and 3D view of the coil lay-out (right).

4.3 Harmonic optimization in a dipole magnets based on sector coils: the low cost of field quality

Let us now compute the multipolar expansion for the sector coil discussed in the previous section. Using the expression computed thanks to the multipolar expansion of a field line, see Chapter 3, Eq. (3.35) and integrating over a sector coil as shown in Fig. 4.5, one finds

$$C_n = -2\frac{\mu_0 jR_{ref}^{n-1}}{2\pi}\int_{-\alpha}^{\alpha}\int_{r}^{r+w}\frac{\exp(-in\theta)}{\rho^n}\rho d\rho d\theta = -\frac{\mu_0 jR_{ref}^{n-1}}{\pi}\int_{-\alpha}^{\alpha}\exp(-in\theta)\,d\theta\int_{r}^{r+w}\frac{d\rho}{\rho^{n-1}}. \tag{4.14}$$

For the second order harmonic one has a logarithmic dependence

$$C_2 = -\frac{2\mu_0 jR_{ref}}{\pi}\sin(2\alpha)\ln\left(1+\frac{w}{r}\right) \tag{4.15}$$

and for the higher orders one has

$$C_n = -\frac{\mu_0 jR_{ref}^{n-1}}{\pi}\frac{2\sin(n\alpha)}{n}\frac{(r+w)^{2-n}-r^{2-n}}{2-n}. \tag{4.16}$$

Summarizing, one finds that

- The unnormalized field harmonics are proportional to the current density;
- The unnormalized field harmonics of order *n* are proportional to the sinus of *n* times the angle of the sector; therefore they can be set to zero with an appropriate selection of the sector angle;
- The unnormalized field harmonics of order *n* are proportional to the inverse of a power *n*-2 of the location of the current lines in the sector; therefore high order multipoles are barely affected by the parts of the coil that are far from the centre.

The 60° degrees sector coil cancels the first order harmonic C_3 since sin 3 π/3 = 0. Note that to cancel out the order five one needs either 36° or 72° degrees sector coil. Obviously, having only one angle to play with, one can cancel only one harmonics. This is why we have to go for sector coils with wedges.

Let us consider a sector coil with one wedge, as shown in Fig. 4.5; the unnormalized multipoles are given by

$$C_n = -\frac{\mu_0 jR_{ref}^{n-1}}{\pi}\frac{(r+w)^{2-n}-r^{2-n}}{2-n}\frac{2}{n}\left[\sin(n\alpha_3)-\sin(n\alpha_2)+\sin(n\alpha_1)\right] \tag{4.17}$$

and therefore there are solutions that can cancel both order 3 and order 5: this corresponds to solving the equation

$$\begin{aligned}\sin(3\alpha_3)-\sin(3\alpha_2)+\sin(3\alpha_1)&=0\\ \sin(5\alpha_3)-\sin(5\alpha_2)+\sin(5\alpha_1)&=0\end{aligned}. \tag{4.18}$$

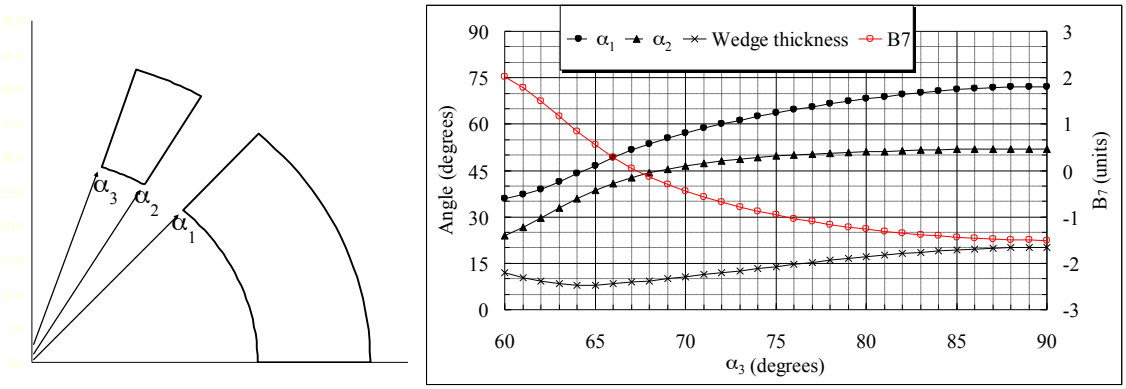

Fig. 4.6: Sector coil with one wedge (left) and solutions of the angles α_1 α_2 as a function of α_3 that set to zero b_3 and b_5 (right).

Four different solutions with integer angles exist, easy to memorize:

- (0°-24°), (36°-60°) this has the lower angular width (total of 48°);
- (0°-36°), (44°-64°) this has the lower angular width of the wedge (8°);

- (0°-48°), (60°-72°) this is widely used by magnet designers;
- (0°-52°),(72°-88°) this is of little practical interest since the winding extends to angles which give very small contribution to vertical field, i.e. is far from being effective in the use of the conductor. Moreover having a winding that extends over nearly 90° poses other challenges in terms of manufacturing and assembly.

The values of α_1 and α_2, as a function of α_3, that solve the system (4.18) are given in Fig. 4.6 right, where also the thickness of the wedge is given, and B_7. There is one value that cancels also B_7: it corresponds to the angles ~(0°-43.2°),(53.2°-67.3°); the layout is shown in Fig. 4.7.

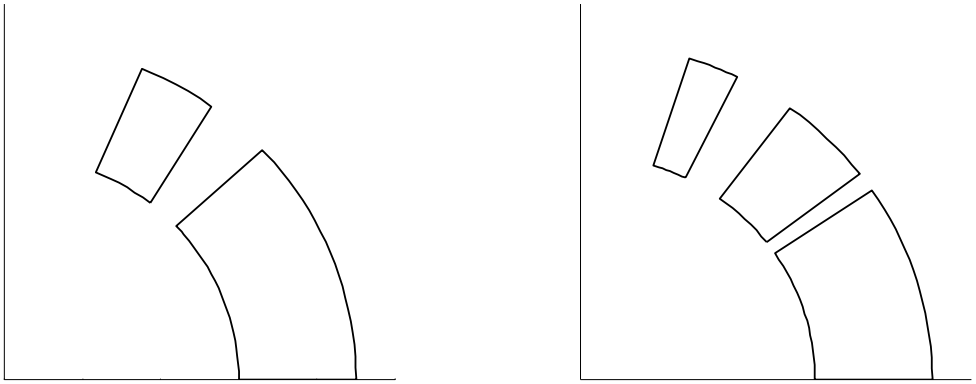

Fig. 4.7: One wedge sector coil canceling up to b_7 (left) and two wedges sector coil canceling up to b_{11} (right).

Now it is easy to generalize to another wedge, to cancel also B_9 and B_{11}: one will have to solve the system

$$\begin{aligned}
\sin(3\alpha_5)-\sin(3\alpha_4)+\sin(3\alpha_3)-\sin(3\alpha_2)+\sin(3\alpha_1)&=0\\
\sin(5\alpha_5)-\sin(5\alpha_4)+\sin(5\alpha_3)-\sin(5\alpha_2)+\sin(5\alpha_1)&=0\\
\sin(7\alpha_5)-\sin(7\alpha_4)+\sin(7\alpha_3)-\sin(7\alpha_2)+\sin(7\alpha_1)&=0\\
\sin(9\alpha_5)-\sin(9\alpha_4)+\sin(9\alpha_3)-\sin(9\alpha_2)+\sin(9\alpha_1)&=0\\
\sin(11\alpha_5)-\sin(11\alpha_4)+\sin(11\alpha_3)-\sin(11\alpha_2)+\sin(11\alpha_1)&=0
\end{aligned} \tag{4.19}$$

that may appear pretty complex, but that can be solved with numerical tools, and has one solution shown in Fig. 4.8 ~(0°-33.3°),(37.1°-53.1°),(63.4°-71.8°).

These simple equations already give a good analytical insight on the angles of the coil selected for the RHIC dipole (see Fig. 4.8), which is a large aperture (80 mm diameter) magnet based on a 10-mm-width sector coil [6]. The angles of the wedges are not far from the analytical solution; moreover the first block is split in two to be able to recover a prependicularity between cables and magnet aperture.

For a two layer magnet things become a bit more complex, since there is a dependency also on radial parameters which is not present in the case of a one layer coil. Let us carry out the computations for a two layer coil, without wedges; we will have two free parameters, namely the angle of the first layer and the angle of the second one (see Fig. 4.9).

In this case, the integration of the contribution of field lines gives

$$C_n = -\frac{2\mu_0 j R_{ref}^{n-1}}{\pi n(2-n)}\left(\left[\frac{1}{(r+w)^{n-2}} - \frac{1}{r^{n-2}}\right]\sin(n\alpha_1) + \left[\frac{1}{(r+2w)^{n-2}} - \frac{1}{(r+w)^{n-2}}\right]\sin(n\alpha_2)\right) \quad (4.20)$$

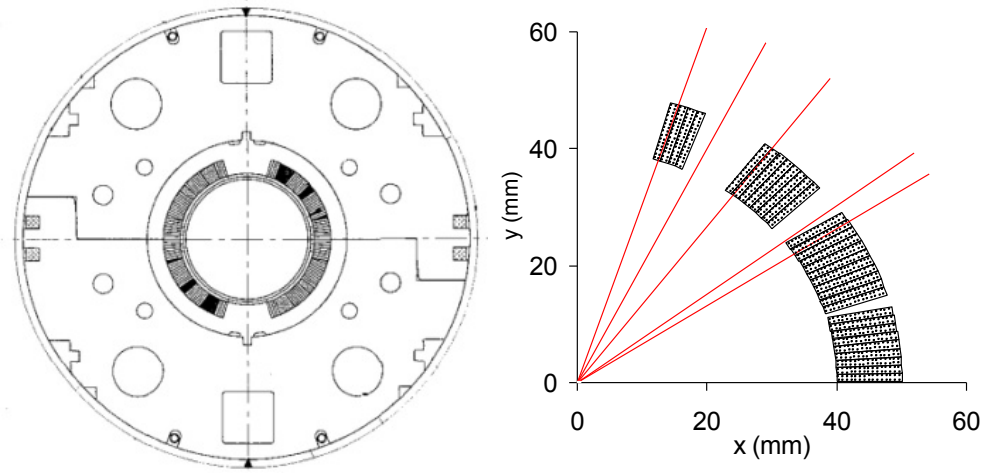

Fig. 4.8: RHIC dipole magnet cross-section (left) and cross-section of the coil (one quarter shown, right) with red lines indicating the angles of coil shown in Fig. 4.7, right.

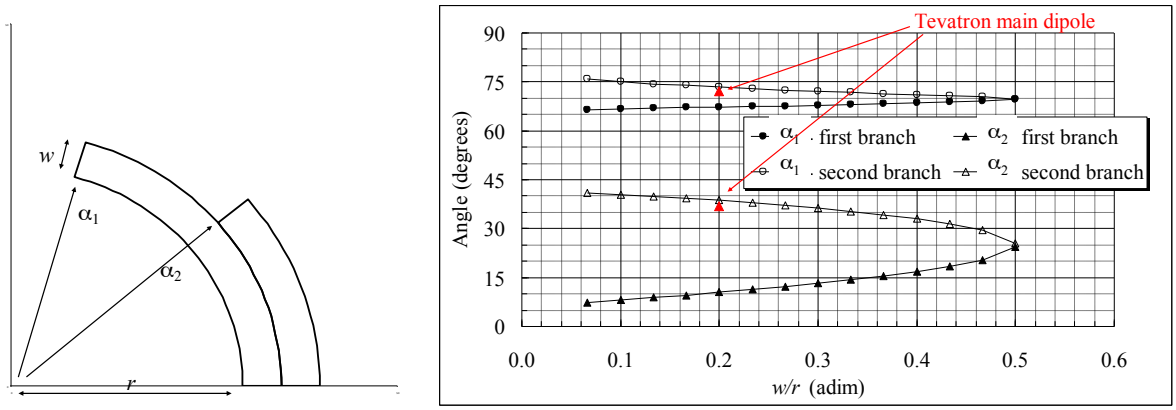

Fig. 4.9: Two-layer coil withhout wedges (left) and solutions setting to zero b_3 and b_5 as a function of the ratio between the layer width and the aperture radius (right)

and the equations to set order B_3 and B_5 to zero are

$$\begin{gathered}\left[\frac{1}{r+w} - \frac{1}{r}\right]\sin(3\alpha_1) + \left[\frac{1}{r+2w} - \frac{1}{r+w}\right]\sin(3\alpha_2) \\ \left[\frac{1}{(r+w)^3} - \frac{1}{r^3}\right]\sin(5\alpha_1) + \left[\frac{1}{(r+2w)^3} - \frac{1}{(r+w)^3}\right]\sin(5\alpha_2)\end{gathered} \quad (4.21)$$

that can be rewritten as

$$\left[\frac{1}{1+w/r}-1\right]\sin(3\alpha_1)+\left[\frac{1}{1+2w/r}-\frac{1}{1+w/r}\right]\sin(3\alpha_2)$$
$$\left[\frac{1}{(1+w/r)^3}-1\right]\sin(5\alpha_1)+\left[\frac{1}{(1+2w/r)^3}-\frac{1}{(1+w/r)^3}\right]\sin(5\alpha_2) \quad (4.22)$$

The numerical solutions that can be computed with any solver are shown in Fig. 4.9, right. For $w/r>0.5$ there are no solutions, since the second layer is too far to inflence B_5. Below this limit there are two solutions, the most interesting of which is the upper branch. Note that Tevatron dipole (see 4.10) has r=43 mm and w=8, i.e. w/r=0.2, and the analytical solution on the upper branch corresponds to ~73° and ~37° for inner and outer layer respectively [7]. It is in very good agreement with the the actual design of the magnet coil, see Fig. 4.10.

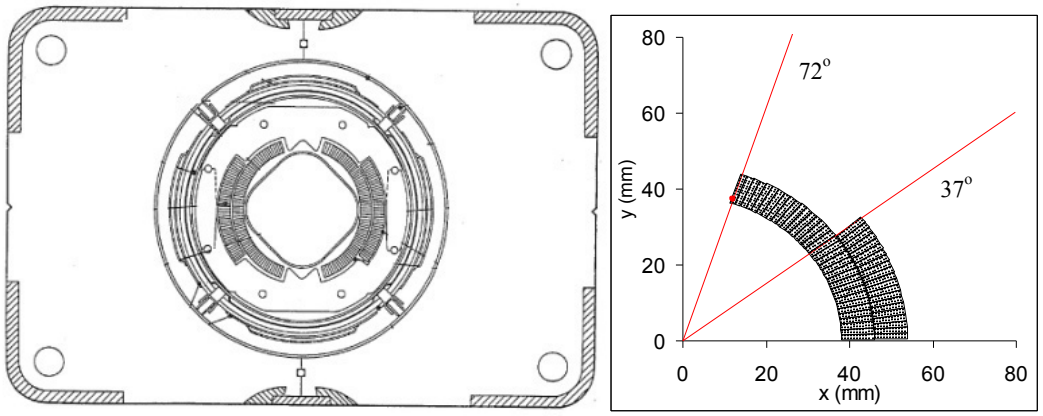

Fig. 4.10: Tevatron dipole magnet cross-section (left) and cross-section of the coil (one quarter shown, right) with angles shown.

In Table 4.1 we compare the proportionality factors between field and coil width times current density. As expected, layouts with larger angular width (i.e. more conductor) provide more field. Having a closer look at the comparison between the (0°-60°) and the (0°-48°),(60°-72°), we see that they have the same angular width (same quantity of conductor) and therefore a direct comparison is possible; setting also b_5 to zero as in the (0°-48°),(60°-72°) solution costs about 5% in terms of field obtained by the same quantity of conductor. The sector coils setting to zero up to order 7 and up to order 11 have a 3% lower constant, but with a 4.5% lower angular width. Note the (0°-52°),(72°-88°) lay-out: the B/jw is the same of the (0°-48°),(60°-72°), layout, but using a 10% larger angle as conductors at very large

Lay-out	B/jw (T mm/A)	Angular width	Field quality
Solenoid	12.56×10^{-4}		all b_n=0
Wall dipole	12.56×10^{-4}		all b_n=0
Cos theta	6.28×10^{-4}		all b_n=0
Intersecting circles	6.28×10^{-4}		all b_n=0
Sector coil (0°-60°)	6.93×10^{-4}	60°	b_3=0
Sector coil (0°-24°),(36°-60°)	5.48×10^{-4}	48°	b_n=0 up to n=5

angles give smaller contribution to the main field.

Sector coil (0°-36°),(44°-64°)	6.34×10^{-4}	56°	b_n=0 up to n=5
Sector coil (0°-48°),(60°-72°)	6.63×10^{-4}	60°	b_n=0 up to n=5
Sector coil (0°-52°),(72°-88°)	6.69×10^{-4}	66°	b_n=0 up to n=5
Sector coil ~(0°-43.2°),(53.2°-67.3°)	6.45×10^{-4}	~57.3°	b_n=0 up to n=7
Sector coil ~(0°-33.3°),(37.1°-53.1°),(63.4°-71.8°)	6.41×10^{-4}	~57.5°	b_n=0 up to n=11

Table 4.1: Ratio between field and coil width times current density, angular widths and field quality for different coil lay-outs.

4.4 Electromagnetic efficiency of coil layouts

In the previous section we compared the electromagnetic efficiency of a coil layout computing the ratio between the field and the current density times the coil width:

$$\frac{B}{jw} \tag{4.23}$$

but we also showed that layouts with same coil widths can have different quantities of conductor, according to the angular width of the sector and of the wedges; for this reason, it is better to define an equivalent coil width by computing the width of a 60° sector coil whose area is the same of the area of the layout that we are considering. This also allows to generalize the concept to any shape of coil [8].

How to define an equivalent coil width ? Since a 60° sector coil has a cross-sectional surface A given by

$$A = \frac{2\pi}{3}\left[\left(r+w\right)^2 - r^2\right] \tag{4.24}$$

and one can invert explicitely the above relation according to

$$\frac{3A}{2\pi r^2} = \left[\left(1+\frac{w}{r}\right)^2 - 1\right] \qquad \sqrt{1+\frac{3A}{2\pi r^2}} - 1 = \frac{w}{r}, \tag{4.25}$$

and if we consider a coil with arbitrary shape and cross-sectional surface A, we can define the equivalent coil width as

$$w_{eq} \equiv r\left(\sqrt{1+\frac{3A}{2\pi r^2}} - 1\right) \tag{4.26}$$

i.e. the width of the 60° sector coil having the same aperture and the same quantity of conductor. Once we have computed this parameter, we can compute

$$\gamma_c \equiv \frac{B}{jw_{eq}} \tag{4.27}$$

and we compare to the value of 6.63×10^{-4} T mm/A found for a coil with one wedge, total angular width 60°, setting to zero first two order harmonics, and having a wedge between 48° and 60°.

Let us start the exercise with the layouts given in the section 4.1. The wall dipole cannot be treated in this way, since it requires an infinite coil. Considering the intersecting ellipses, we have to compute the area of the coil, find the equivalent coil width and estimate the coefficient γ_c using the relation for

the magnetic field (4.4). The layout depends on two parameters: the ratio between the axis and the width of the coil in the midplane. Results are shown in Fig. 4.11, for an aperture radius of 25 mm: the intersecting ellipses layout can provide values between 6.5×10^{-4} and 7.0×10^{-4} T mm/A, i.e. up to 6% larger than the sector coil with one wedge. The price to pay for this larger efficiency is a larger coil width in the midplane (see case in Fig. 4.12, refering to 40 mm equivalent coil width, and giving a 50 mm coil width in the midplane) and the presence of conductor at angles close to 90°, not trivial to integrate in a mechanical structure.

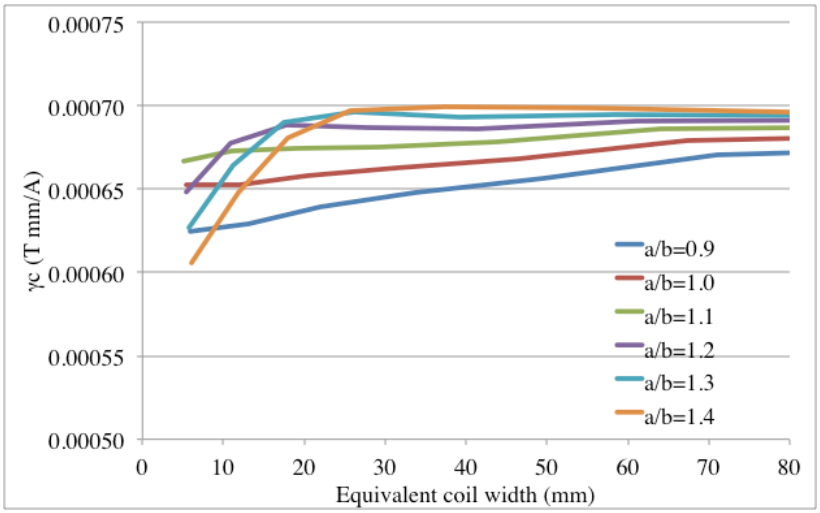

Fig. 4.11: Coil efficiency for intersecting ellipses lay-outs.

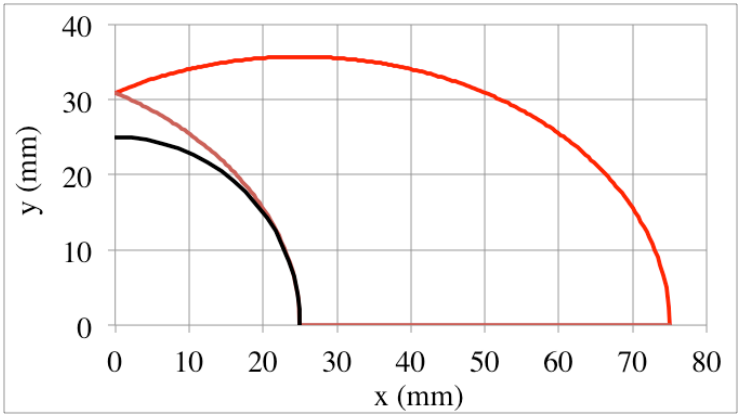

Fig. 4.12: One quarter of coil in the most efficient intersecting ellipses layout for a 40 mm coil width and 25 mm aperture radius, having a γ_c close to 0.00070 T mm /A. Winding contour in red, aperture in black.

The second case is the cosθ layout. Here in principle one should take the whole ring as conductor area, but the current density is not uniform; therefore, we assume that the full current density is gathered in a sector of angle α,

$$\int_0^{\pi} \cos\theta \, d\theta = \int_0^{\alpha} d\theta \tag{4.28}$$

thus giving α=1 (in radiants), i.e. a 5% smaller angular width of $\pi/3$. Estimating the efficiency for a few coil widths, and a aperture radius of 25 mm, we find values around 6.5×10^{-4} T mm/A, i.e. very close to our reference value of a sector coil with one wedge.

Using the same approach, we can estimate the efficiencies of the layouts whose total angular width is not exactly 60°; here the efficiency computation weakly depends on the ratio between the coil width and the aperture radius – we present in Table 4.2 few cases. Values are very similar, and for the cases range with field quality correction up to order 7 or 11 the efficiency is in a narrow range between 6.6 and 6.7×10^{-4} T mm/A.

Table 4.2: Coil efficiencies as defined in (4.27)

Coil efficiency (T mm/A)	*r=25 mm* *w=10 mm*	*r=25 mm* *w=30 mm*	*r=25 mm* *w=50 mm*
Cos theta	6.53×10^{-4}	6.49×10^{-4}	6.48×10^{-4}
Intersecting circles (best case)	6.77×10^{-4}	6.99×10^{-4}	6.98×10^{-4}
Sector coil (0°-60°)	6.93×10^{-4}	6.93×10^{-4}	6.93×10^{-4}
Sector coil (0°-24°),(36°-60°)	6.65×10^{-4}	6.46×10^{-4}	6.37×10^{-4}
Sector coil (0°-36°),(44°-64°)	6.73×10^{-4}	6.67×10^{-4}	6.64×10^{-4}
Sector coil (0°-48°),(60°-72°)	6.63×10^{-4}	6.63×10^{-4}	6.63×10^{-4}
Sector coil ~(0°-43.2°),(53.2°-67.3°)	6.71×10^{-4}	6.67×10^{-4}	6.65×10^{-4}
Sector coil ~(0°-33.3°),(37.1°-53.1°),(63.4°-71.8°)	6.65×10^{-4}	6.61×10^{-4}	6.59×10^{-4}
Best efficiency	7.33×10^{-4}	7.20×10^{-4}	7.13×10^{-4}
Tevatron dipole	6.89×10^{-4}		
LHC dipole (removing grading)	6.57×10^{-4}		
MDPTC1 (removing grading)	6.61×10^{-4}		

Is it possible to have a better layout ? A recent work [9] shows that the answer is affirmative. Considering an arbitrary path around a round aperture of radius *r*, and imposing a perfect field quality, one can select the best layouts providing the highest field for a given coil surface and current density. The shapes of the most efficient layouts are intriguing, see Fig. 4.13. As observed in the paper, for smaller coil width the optimal solution is not far from an intersecting ellipses. For large coil widths, the optimal shape becomes more complex. As for intersecting ellipses or cos theta layout, the configurations shown in Fig. 4.13 are not windable with a rectangular or a trapezoidal cable. However, the plot is extremely interesting since it sets the reference for the maximum efficiency, that ranges from 7.1 and 7.4×10^{-4} T mm/A, i.e. about 10% more than the sector coils (see Table 4.2). We add in the Table also the efficiencies computed for the Tevatron dipole, and for the LHC dipole [10] and the MDPCT1 dipole model [11] (in both cases removing the grading, i.e. placing the same current density in all layers). Results range from 6.6 to 6.9×10^{-4} T mm/A: this shows how the sector coil is close to what can be achieved in real dipole coils.

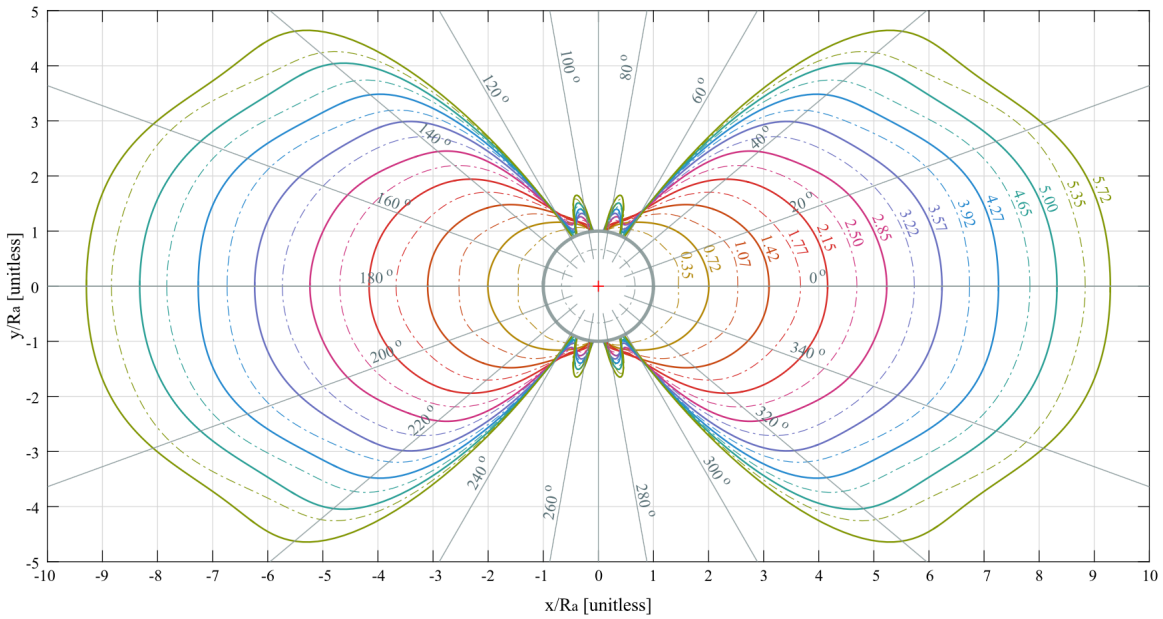

Fig. 4.13: Shapes of the most efficient coil lay-out, from [9]

4.5 Efficiencies of block and double helix layouts

Tevatron and RHIC dipole coils have a width of 10-15 mm, and a ratio between the coil width and the aperture radius of the order of 0.2. Dipoles for higher energy accelerators have a smaller aperture, and possibily also higher field. In the LHC dipole, with a 56 mm aperture diameter and 31 mm coil width based on double layer coil, the ratio *w*/*r* is around 1. In this case the second layer has a lower angle, since it is equivalent to place the precious conductor in the midplane at the edge of the coil, or on the top of a closer layer (see Fig 4.14 left): the first configuration is mechanically more stable, and the efficiency is not compromised. The angles of the outer layers provide also a good way to steer field quality for the low order multipoles, as done in the Tevatron coil, and they are decoupled to the high order multipoles. The same approach has been used for the four layers dipole MDPCT1 (Fig. 4.14, right).

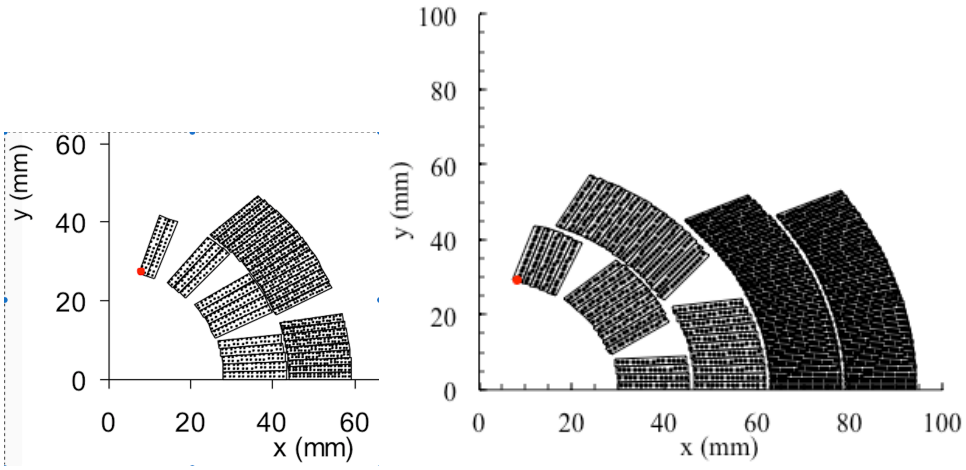

Fig. 4.14: Main LHC dipole magnet cross-section (left), and MDPTC1 dipole magnet cross-section (right).

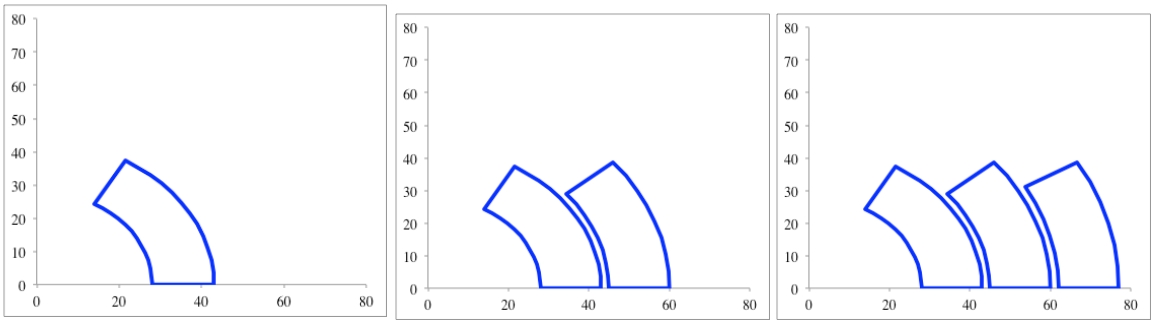

Fig. 4.15: Dipole coils based on sector with additional layers and decreasing angles

When the coil width becomes very large with respect to the aperture radius, the natural configuration of the coil tends to a solution whose contour looks like a rectangular coil rather than a sector coil (see Fig. 4.15). This trend is also visible in the optimal layout as shown in Fig. 4.13. This is the configuration that can be achieved in a block coil [13]. Note that compared to sector layouts, block coils are based on a radically different concept:

- the cable is wound perpendicular to the midplane; therefore it is rectangular and in the straight part of the magnet the coil is a flat racetrack;
- There is no arc structure and therefore one needs to have in internal structure to support the upper deck;
- The coil ends are flared to free the space needed to thebeam tube.

The case of the HD2 dipole [13] is shown in Fig. 4.16. The layout is extremely simple, requiring a cable width of the order of the magnet aperture (22 mm cable width for an aperture radius of 17.5 mm). The design was also generalized to four decks in the case of Fresca2 (see Fig. 4.17), where the cable width is 20 mm, on two layers per deck, for the 50 mm free aperture [14]. An advantage of this layout is that the amount of conductor can be gradually increased (up to a certain extent, given by field quality constraints), whereas in the sector coil it is quantized by the number of layers. A design based on three layers, i.e. relying on a total of three coils per dipole, has been used in RMM, a cell dipole with 50 mm aperture aiming reaching a bore field above 16 T [15], see Fig. 4.18.

The field quality is guaranteed by having the upper deck of the coil closer to the magnet vertical axis. Good field quality can be achieved without wedges, as in HD2 or in FrescaII layouts: the three free parameters are the cable height, the indent of the upper deck, and the width of the decks. An essential point is that there is no arch structure and therefore a support of the upper deck is needed to avoid its collapse on the aperture. This is taking some space in the aperture: for the design shown below, the HD2 has a free aperture of 17.5 mm radius, and FrescaII has 50 mm radius. The efficiency γ_c of the coil is 5-10% lower than in sector coils, but the efficiency approaches the sector coil for larger and larger ratios coil width/aperture width: it is 5.9×10^{-4} T mm/A for HD2, 6.1×10^{-4} T mm/A for FrescaII, and 6.4×10^{-4} T mm/A for RMM.

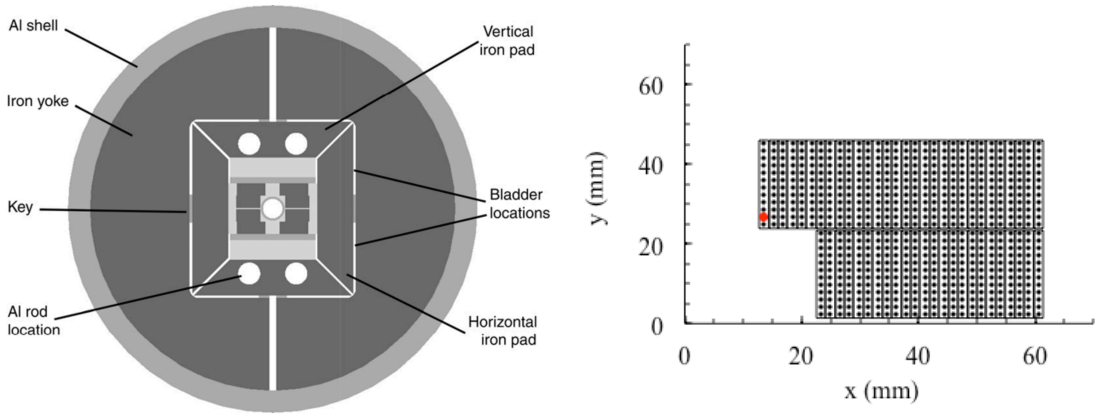

Fig. 4.16: Cross-section of HD2 dipole (left) and of its coil (right)

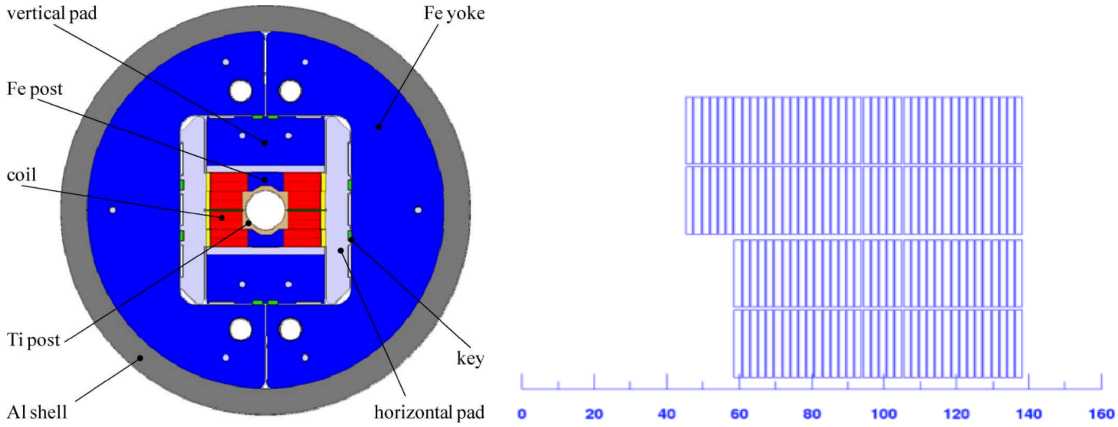

Fig. 4.17: Cross-section of FrescaII dipole (left) and of its coil (right).

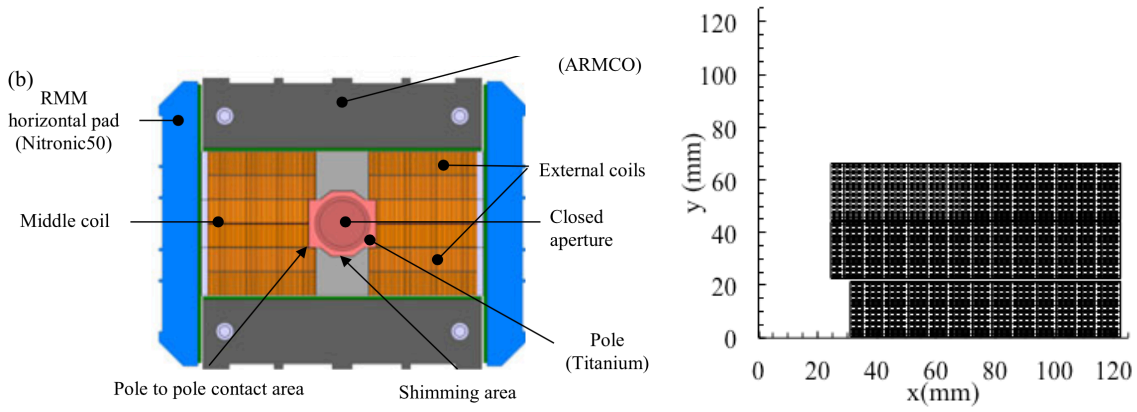

Fig. 4.18: Cross-section of RMM dipole (left) and of its coil (right).

We conclude with section with an exercise to estimate the efficiency of the double helix layout, that is lower than the sector coil by at least the factor cos α.

Example 4.1: The D2 corrector [15] in the HL-LHC project is based on double helix design, with an angle α of 30 degrees. It requires 8800 m of 0.825 mm strand, for a double aperture magnet. The aperture diameter is 105 mm, and the diameter of the insulated strand is 1 mm. Ten wires are wound in

a slot with 2.1 mm width and 5.1 mm height. The magnet operates at 392 A giving 2.62 T over 1.92 m of magnetic length. In case of single coil configuration, the field at 392 A is 1.7 T. Compute the coil efficiency of this layout.

The total volume of the insulated coil is $4.4\times10^6/10\times5.1\times2.1=9.42\times10^6$ mm^3. Since there are two apertures and the magnetic length is 1.92 m, the cross-section area is 2454 mm^2. Using the definition of equivalent coil width one finds

$$w_{eq} = r\left(\sqrt{1+\frac{3A}{2\pi r^2}}-1\right) = 52.5\left(\sqrt{1+\frac{3\times2453}{2\pi\left(52.5\right)^2}}-1\right) = 10.16\text{mm} \tag{4.29}$$

Since the current density is 4920/5.1/2.1=459 A/mm^2, the efficiency is $1.7/10.16/459=3.64\times10^{-4}$ T A/mm, i.e. 55% of the efficiency of a sector winding. Note that the geometric factor of loss due to the angle of 30° is cosα=0.87.

4.6 Field quality optimization for quadrupoles based on sector coils

We now consider the case of a quadrupole magnet, as discussed in [4]. In this case the four sectors are arranged around the aperture, with current signs alternating. The integration of the second order contribution gives (see 4.10)

$$\frac{B_2}{R_{ref}} = -\frac{2\mu_0 j}{\pi}\sin(2\alpha)\ln\left(1+\frac{w}{r}\right) \tag{4.30}$$

and considering a 30° degrees sector coil one finds

$$G \equiv \frac{B_2}{R_{ref}} = -\frac{\sqrt{3}\mu_0 j}{\pi}\ln\left(1+\frac{w}{r}\right) \tag{4.31}$$

and using the more comfortable units

$$G = -\frac{\sqrt{3}\times4\pi\times10^{-7}}{\pi}10^6\, j\left[\text{A/mm}^2\right]\ln\left(1+\frac{w}{r}\right) = 0.69\, j\left[\text{A/mm}^2\right]\ln\left(1+\frac{w}{r}\right). \tag{4.32}$$

For instance, in the LHC main quadrupole one has a 440 A/mm^2 current density, and a coil width of 31 mm similar to the aperture radius of 28 mm. Therefore one finds

$$G = 0.69\times440\times\ln\left(1+\frac{31}{28}\right) \approx 0.69\times440\times0.75 = 220\ \text{T/m}. \tag{4.33}$$

The equations for the field quality optimization are very similar to the dipole ones, provided that (i) angles are divided by a factor two and (ii) multipole orders are multiplied by a factor 2. Therefore a coil layout with one wedge can cancel both B_6 and B_{10} provided that the wedge angles satisfy the equation

$$\begin{aligned}\sin(6\alpha_3)-\sin(6\alpha_2)+\sin(6\alpha_1)=0\\ \sin(10\alpha_3)-\sin(10\alpha_2)+\sin(10\alpha_1)=0\end{aligned}. \tag{4.34}$$

The integer solutions of interest for quadrupole layout, canceling b_6 and b_{10}, are

- (0°-12°), (18°-30°);

- (0°-18°), (22°-32°);
- (0°-24°), (30°-36°).

Field quality optimization is much easier in quadrupoles, since the the non zero orders are more spaced (a quadrupole has only two multipoles to cancel up to order 10, i.e. b_6 and b_{10}, whereas a dipole has b_3 b_5 b_7 and b_9), and even the cross-section of two layers quadrupoles can be easily interpreted according to the solutions given above.

For instance, the LHC quadrupole has an inner layer based on the (0°-24°), (30°-36°), and the outer layer on a 30 degrees sector, where the wedge is needed just for placing the conductors back to a perpendicular positions (see Fig. 4.19, left). The 30 degrees layout does not cancel B_{10}, but since the cable width is large, the outer layer is so far from the aperture that its influence on B_{10} is negligible.

As a second case, let us consider the Tevatron main quadrupole: here the inner layer follows the (0°-12°), (18°-30°) layout, and the outer layer is a 30° wedgeless sector coil, as also in this case the influence of the outer layer on B_{10} is negligible (see Fig. 4.19, right).

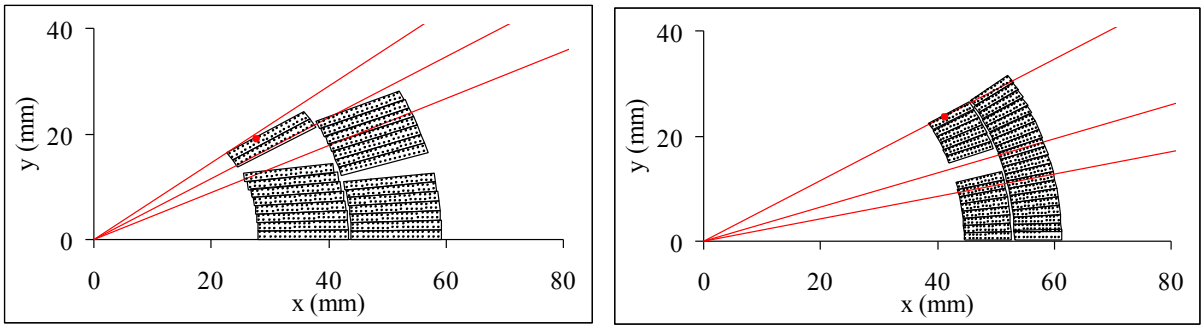

Fig. 4.19: Cross-section of LHC quadrupole coil, with 24°, 30° and 36° angles indicated in red (right). Cross-section of Tevatron quadrupole (left) and of its coil, with 18°, 24° and 30° angles indicated in red (right).

4.7 Guidelines for field quality optimization

Field quality optimization is a bit more complex than what shown in the previous sections. On the top of the geometric contribution discussed in this chapter, at low currents the magnetization of the superconductor can perturb the field harmonics, especially if the energy increase of the accelerator is large and therefore the main magnet are used at injection with very low currents; the phenomena of magnetization will be discussed in Chapter 6. The iron also plays a relevant role, and will be treated in Chapter 9; its influence on field and harmonics can be derived for some shapes in the case of non saturated domains, via the image current method. However, when the iron becomes saturated, finite element methods should be used to compute its impact on the main field and on the harmonics. One of the most used codes is ROXIE (see [16] for the first reference to the initial phase of this fundamental software, and [17] for the dedicated web site), a code dedicated to accelerator magnets developed at CERN by S. Russenschuck and collaborators, including also optimization routines, quench protection estimates. OPERA [18], a commercial code, is also widely used in the community for a vast range of applications. The perturbation induced by iron saturation on harmonics can be minimized via a proper shaping of iron. Both persistent currents and iron saturation are second order effect with respect to the geometric contribution. Therefore, the problem of field quality can and should be sliced, and the geometric part for a dipole should be the first and the more complex slice to swallow. No point in playing with iron shape if the coil geometry is not well optimized.

We have seen that for the geometrical contribution there are five parameters to be optimized (b_3 to b_{11}). The safest method is to first look for a coil layout that provides a good field quality (all multipoles within a few units), forgetting about iron saturation, superconductor magnetization, and just using the Biot-Savart contribution. Each block has in principle three free parameters: the angular position of the lower cable ϕ, the number of conductors, and the inclination of the block α (see Fig. 4.20). However, the third parameter has a very limited range, and the second is quantized by the finite thickness of the cable. Therefore with two wedges (three blocks) one can have not enough flexibility to optimize field quality. Three wedges (four blocks) can provide the needed flexibility, and four wedges (five blocks) provide an additional couple of free parameter that can turn out to be very useful in finding more efficient and flexible solutions.

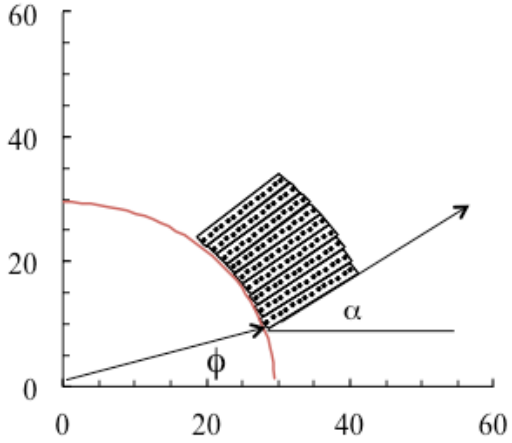

Fig. 4.20: The two angles ϕ and α giving the position of a coil block according to ROXIE nomenclature.

If you have two layers, also in this case three wedges (five blocks) could be enough, usually split bewteen two in the inner layer and one in the outer. Four wedges provide a much larger flexibility, and is the solution adopted for the SSC prototypes and for the final design of the LHC dipoles. However, LHC dipole prototype using five blocks were also manufactured.

When you have two layers, start minimizing the higher orders with the inner layer, and then tune the outer layer to set to zero also b_3 and b_5. In general, a layout with well optimized high orders can be fine tuned to achieve any required large variations of low orders without spoiling the optimization. On the other hand, if you start with a solution with a wrong high order (i.e. 50 units of b_9), it is very difficult to find a solution in its neighbourhood with zero units of b_9, and you will have to start your optimization from scratch.

Once you have found a good single aperture ironless cross-section given the aperture and the cable size, increase the complexity adding the second aperture (if the magnet is two in one) and the iron. The multipoles will move a bit from the target, and to compute how much you will need to run a finite element code with all the detail of the geometry. Once you have the offset that you need to correct, go back to your Biot-Savart model, make a sensitivity matrix of the multipoles on the wedge position, and try to solve the inverse problem. Since the computation of the Biot-Savart contribution takes a fraction of second, whereas a full finite element code can take minutes, this approach can be much faster and also gives you some analytical insight.

Fully automated methods to find the optimal field quality exist, and they are based on a optimizer associated to the algorithm of evaluation. The main difficulty of these methods is related to the existence of local minima for a parametric space that has several dimensions. The slicing technique

allows avoiding taking the problem in the full complexity or, in the language of a mathematician, to diagonalize the problem. On January 20, 1961, John Fitzgerald Kennedy said in his inaugural address "Ask not what your country can do for you – ask what you can do for your country." Talking about field quality optimization, I would suggest: "Ask not what your computer can think for you, ask what you can think for your computer."

Acknowledgements

I wish to thank L. Rossi, who in 2006 suggested me to explore the analytical approaches to magnetic design using the model of the sector coils, and for the all the work carried out together about dipoles and quadrupoles magnetic design.

References

1. M. N. Wilson, "Superconduting magnets" Claredon Press (1987)
2. K.-H. Mess, P. Schmuser, S. Wolff, "Superconducting accelerator magnets" World Scientific, Singapore (1996)
3. L. Rossi, E. Todesco, "Electromagnetic design of superconducting dipoles based on sector coils", Phys. Rev. STAB 10 (2007) 112401
4. L. Rossi, E. Todesco, "Electromagnetic design of superconducting quadrupoles", Phys. Rev. STAB 9 (2006) 102401
5. D. I. Meyer and R. Flasck, "A new configuration for a dipole magnet for use in high energy physics applications" Nucl. Instrum. Meth. 80 (1970) 339-341
6. M. Anerella, et al., "The RHIC magnet system" Nucl. Instrum. Meth. A 499 (2003) 280-315
7. R. Palmer and A. V. Tollestrup, "Superconducting magnet technology for accelerators" Ann. Rev. Nucl. Part. Sci. 34 (1984) 247
8. L. Rossi, E. Todesco, "Electromagnetic efficiency of block design in superconducting dipoles" IEEE Trans. Appl. Supercond. 19 (2009) 1186-1190
9. J. v. Nugteren, et al "Idealized coil cross-sections with minimized conductor area for high field dipoles" IEEE Trans. Appl. Supercond. 28 (2018) 4000205
10. R. Perin, in *Encyclopedia of Applied Superconductivity* (IOP, London, 1998), pp. 919–950
11. A. Zlobin, et al. "Design concept and parameters of a 15 T Nb3Sn dipole demonstrator for a 100 TeV hadron collider" International Particle Accelerator Conference (2015) 3365-3367
12. G. L. Sabbi, et al., "Design of HD2: a 15 tesla Nb3Sn dipole with a 35 mm bore" IEEE Trans. Appl. Supercond. 15 (2005) 1128-1131
13. A. Milanese, et al., "Design of the EuCARD high field model dipole Fresca2" IEEE Trans. Appl. 22 (2012) 4002604
14. S. Izquierdo Bermudez, et al. "Design of ERMC and RMM, the base of the Nb3Sn 16 T magnet development at CERN" IEEE Trans. Appl. Supercond. 27 (2017) 4002004
15. G. Kirby, et al., "Hi-Lumi LHC twin aperture orbit correctors magnet system optimisation" IEEE Trans. Appl. Supercond. 27 (2017) 4002805
16. S. Russenschuck, T. Tortschanoff, "Mathematical optimization of supeorconducting accelerator magnets" IEEE. Trans. Magn. 30 (1994) 3419-3422
17. www.cern.ch/roxie
18. Vector Fields, "OPERA-2d & 3-d User Guide ", Vector Fields Limited, England, 1999